J. Physiol. (1956) 134, 451–470

STIMULATION OF SPINAL MOTONEURONES WITH INTRACELLULAR ELECTRODES

By K. FRANK and M. G. F. FUORTES

From the Laboratory of Neurophysiology, National Institutes of Health, Bethesda, Maryland, and the Department of Neurophysiology, Walter Reed Army Institute of Research, Walter Reed Army Medical Center, Washington, D.C., U.S.A.

(*Received* 2 *July* 1956)

Some problems of spinal cord function might be clarified if one could distinguish the features of transmission attributable to properties of the motoneurone soma membrane itself from the features attributable instead to properties of such other structures as presynaptic terminals, dendrites or axons. This question can be partly answered by determining the properties of reaction of post-synaptic structures to directly applied stimuli.

Stimulation through intracellular microelectrodes is particularly advantageous because it is then safe to consider that both stimulation and recording are strictly limited to the unit under consideration. In its application to spinal motoneurones this method has been recently employed by Coombs, Eccles & Fatt (1955*a*) and by Araki & Otani (1955).

Using double-barrelled microelectrodes, Coombs *et al.* (1955*a*) have applied stimulating currents through one barrel and recorded the resulting potential changes through the second. In this way the major resistances are independent in stimulating and recording channels, but these are linked together by a considerable capacity. Using this method, motoneurone resistance was found to vary between 0·4 and 1 MΩ. From other measurements a time constant of 4 msec was calculated and a capacity of 4000 pF was ascribed to the motoneurone membrane. Motoneurone excitation occurred when applied stimuli depolarized the membrane by about 10 mV.

Araki & Otani (1955) preferred instead to apply electrical stimuli to the same intracellular electrode used for recording, and employed a bridge circuit for balancing out the potential difference developed across the microelectrode resistance by the stimulating current. With this method, the artifacts due to capacity of double-barrelled electrodes are avoided, but other difficulties are

introduced (see below). In motoneurones of toads, Araki & Otani (1955) measured membrane resistance of 3–6·4 MΩ, time constants of 1·5–8 msec and capacities of 630–1500 pF. Rheobasic currents were $0{\cdot}8–4 \times 10^{-9}$ A.

The present paper describes the results obtained so far by applying a method similar to that used by Araki & Otani (1955) to the study of the electrical properties of cat motoneurones.

METHODS

Twenty-five cats were used for this research. Most of these were anaesthetized with pentobarbitone sodium and a few were decerebrated. Anaesthesia helps to stabilize the properties of penetrated motoneurones and to simplify the preparation. It is recognized, however, that anaesthesia also limits the validity of the results, as it greatly affects the properties of transmission in the spinal cord.

KCl-filled micropipettes were inserted in spinal cord motoneurones and the potentials led off from these elements were amplified and recorded using the technique described in detail in a previous paper (Frank & Fuortes, 1955). In addition, currents were passsed through the same microelectrode used for recording, with the purpose of stimulating penetrated elements directly. Micropipettes initially measuring 5–20 MΩ in 3 M-KCl were preferred to the higher resistance pipettes (15–50 MΩ) used in previous work. With these lower resistance pipettes, penetration of axons occurred only rarely and the percentage of penetrated cell somata was larger than in the previous study (Frank & Fuortes, 1955).

Bridge circuit. The circuit used for balancing the potential drop evoked by stimulating currents is shown in Fig. 1 A. Of the two variable resistances in the lower limb of the bridge only R_2 is normally changed for balancing, adjustment of R_1 being required only if the electrode resistance is less than 4·4 MΩ. The two pulse generators used for stimulation and calibration respectively are isolated from ground, and the cat itself (I.E.) is connected to ground only through the three resistances Cal., Comp., and R_1.

Compensation. The driven shield around the 44 MΩ resistance and part of the microelectrode permits positive feed-back and is designed to improve frequency response and control of stimulus artifacts (see Solms, Nastuk & Alexander, 1953; Woodbury, 1953; MacNichol & Wagner, 1954). The low capacity pre-amplifier input switch (Sw.) permits adjustment of the current through the microelectrode to zero. To accomplish this, the variable resistance (Comp.) is adjusted until no change of output potential occurs when Sw. is moved from closed to open.

Calibration. When the amplifier is not connected to a bridge, its high input impedance makes the input signal independent of electrode resistance. With the bridge shown in Fig. 1 A, the potential between micro- and indifferent electrodes is divided between the electrode resistance R_e and the 44 MΩ resistance R_3 (other resistances being negligible in comparison). Since electrode resistance may change with current through it, with movement of the electrode (see p. 463) and perhaps for other reasons, biological potentials can be measured only if they are compared within a short time (preferably within a few msec) to a known signal. For this purpose a calibration pulse (Cal.) can be displayed on each sweep of the cathode-ray oscilloscope (*CRO*). Comparison of the recorded calibration pulse with Sw. open or closed permits measurement of electrode resistance, as described in a previous article (Frank & Fuortes, 1955).

Current measurement. When R_2 is adjusted for bridge balance, current in the microelectrode can be measured by the potential drop across R_2 which is then equal to the potential drop across R_3. Measurement of microelectrode current from the potential drop across R_2 permits use of a commercially available single-ended amplifier but is in error if the bridge is unbalanced.

Towards the end of this research two high-impedance single-ended pre-amplifiers, similar to that described by MacNichol & Wagner (1954), have been used to measure microelectrode current more directly (Fig. 1 B). Amplifier *V* records the microelectrode potential and amplifier *I* the current

through it by the potential drop across the 5 MΩ resistor R_4. The gains of the pre-amplifiers V and I are adjusted to be equal and are connected as shown to two Tektronix Type 112 final amplifiers. Amplifier V is used single ended and amplifier I with push-pull input connexion. Considerable care is necessary in arranging the driven shields of the two pre-amplifiers to prevent loss of frequency response and good transient control for applied pulses. With this caution the method proved more satisfactory than the first method described since the current was correctly indicated even in the presence of bridge unbalance.

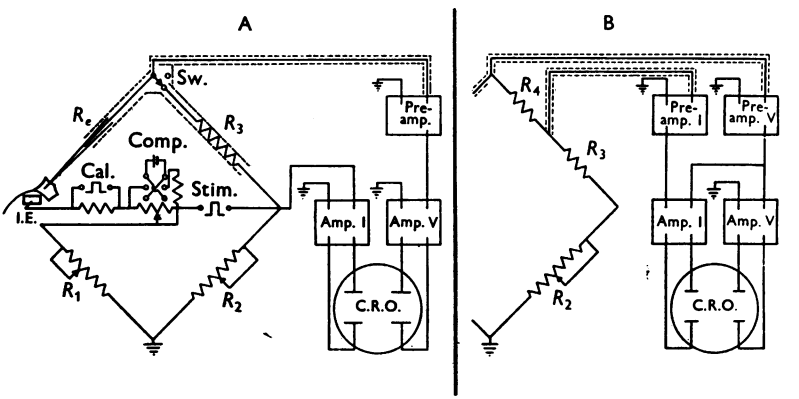

Fig. 1. A: diagram of arrangement used for stimulating and recording. The values of the resistors used are as follows: R_1, 1 kΩ; R_2, 10 kΩ; R_3, 44 MΩ. Electrode resistance R_e usually was between 10 and 100 MΩ when measured in the spinal cord. The resistor of the calibrator (Cal.) and the variable resistor of the compensator (Comp.) are 100 Ω each. The fixed resistor of the compensator has a value of 300 Ω and the battery supplies 1·5 V. Stimulating and calibrating pulses are applied through radio-frequency stimulus isolation units. The indifferent electrode, I.E., is a silver-silver chloride wire and is usually placed in the cat's mouth. The switch, Sw., is used for d.c. compensation and for measurement of R_e, as described in the text. Stimulating current is measured by the voltage drop across R_2, which is equal to the drop across R_3 when the bridge is balanced. B: alternative method for measuring current. R_2 and R_3 (as well as other components not illustrated) are the same as in 1A. R_4 has a value of 5 MΩ, and two pre-amplifiers of equal gain are used for differential recording of the voltage drop across R_4.

RESULTS

Rheobasic current intensity

In agreement with Coombs *et al.* (1955*a*) and with Araki & Otani (1955), it was found that if strong enough currents can be made to flow through the impaling microelectrode in a direction adequate to depolarize the motoneurone membrane (microelectrode positive), excitation of the penetrated unit occurs (Fig. 2A). Depolarizing currents insufficient to excite facilitate the action of orthodromic stimuli (Fig. 2B, C), as well as antidromic invasion of motoneurones (Fig. 3).

Rheobasic currents differ widely in individual units, varying between 2·0 and 18·1 $\times 10^{-9}$ A in the 18 motoneurones of Table 1. This variability can be readily accounted for if one accepts that motoneurones fire an impulse when the polarization of their membrane is decreased to a critical

level to be called 'threshold polarization', V_{th} (Fig. 4). First, the membrane polarization V_m is likely to be more or less removed from the threshold polarization V_{th} in individual motoneurones, for instance, owing to more or less effective background synaptic bombardment. Therefore, even if all motoneurones had similar membrane resistance, different currents would be required to depolarize different motoneurones to their threshold levels. Secondly, the total resistance of the soma membrane is probably quite different in individual units, as a result of the wide variation of their size, for if resistance per unit area is uniform, total resistance is inversely proportional to the membrane area. Consequently more current would be required to evoke a given depolarization in a large motoneurone than in a small one. Finally, the amount of leak around the microelectrode shaft may be a factor of importance.

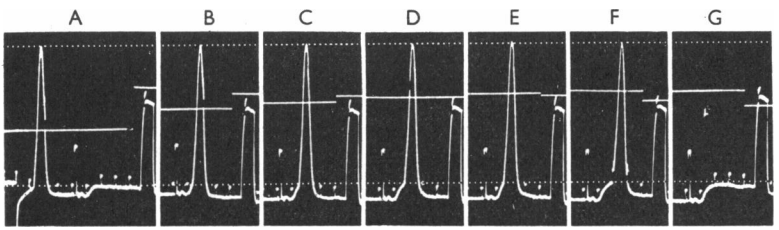

Fig. 2. Effects of currents on orthodromic excitation. Upper trace measures current strength through microelectrode but not timing of current pulse because the sweeps of the two beams were not synchronized. Upward deflexion indicates depolarizing current. Lower trace shows potential of microelectrode after alignment of spike peaks. A calibrating pulse of 50 mV is displayed in each sweep. Time, 1 msec. A: suprathreshold depolarizing current evokes firing with 1·3 msec latency. Subsequent dorsal root stimulus evokes then only a small synaptic potential. With decreasing depolarizing currents (B and C) the synaptic potential becomes more and more evident, approaching its normal height without current (D). With hyperpolarizing currents (E and F) synaptic potential height is increased and firing is delayed. Further increase of hyperpolarizing currents (G) prevents firing. The two horizontal broken lines emphasize approximate constancy of V_{ov}–V_{th} with changing currents (see diagram of Fig. 4).

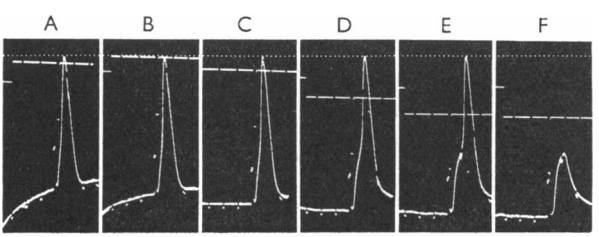

Fig. 3. Effects of currents on antidromic invasion. Upper trace measures current intensity as in Fig. 2. Spike peaks aligned horizontally. Spike height V_s is decreased by depolarizing currents (A and B) and increased by hyperpolarizing currents (D and E). The inflexion in the rising phase of the normal antidromic spike (C) is less prominent during depolarization and more prominent during hyperpolarization, until block occurs (F). Time, 1 msec.

As one would expect, hyperpolarizing currents exert an action opposite to that of depolarizing currents. Orthodromic volleys which safely evoke firing in resting conditions become subthreshold if the motoneurone is hyperpolarized by current flow (Fig. 2 D–G). The inflexion normally present in the rising phase

of motoneurone soma spikes evoked by antidromic stimuli (Brock, Coombs & Eccles, 1953; Frank & Fuortes, 1955) is emphasized by weak hyperpolarizing currents, and for stronger current intensity the motoneurone spike falls from the point of inflexion (Fig. 3 D–F). The values of current intensity eliciting this 'partial block' of antidromic spikes are given in Table 1, column 3.

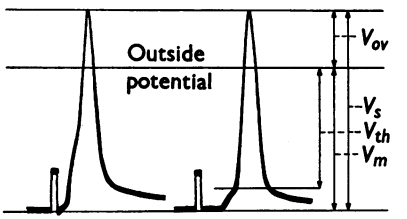

Fig. 4

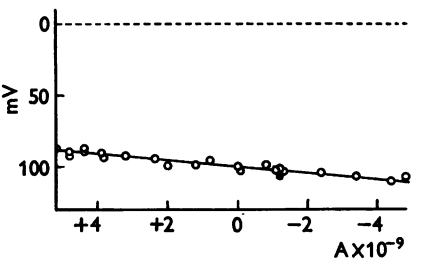

Fig. 5

Fig. 4. Diagram to illustrate terminology used with reference to antidromic or orthodromic action potentials. All potentials are measured from the outside potential taken as 0. V_{th} (which can be measured only for orthodromic spikes) and V_m are negative quantities. V_{ov} and $V_s = V_{ov} - V_m$ are positive quantities.

Fig. 5. Plot of antidromic spike height (V_s) as a function of current through microelectrode. V_s plotted downward from broken line to indicate assumption that the spike peak potential V_{ov} is unaffected by current. Positive current is outward directed. Data from records like those of Fig. 3. Slope is 2·3 MΩ. Note that zero of potential scale is *not* outside potential on this and subsequent plots.

Membrane resistance and threshold polarization

Since the potential drop occurring across the membrane as a result of current is balanced out by the bridge together with the larger potential drops across other resistances, the potential of the membrane cannot be measured directly during current flow. Threshold polarization and membrane resistance were determined therefore by two indirect methods. It will be seen that both methods are subject to certain limitations but these do not include dependence of the results on resistance of the cytoplasm.

Spike height (V_s) method. The first method is based upon measurement of spike height ($V_s = V_{ov} - V_m$) during flow of polarizing currents (see Fig. 4). Within limits the rate of change of resting polarization, V_m, with current can be taken to measure the resistance R_m of the resting membrane. Thus

$$dV_m/dI = R_m.$$

If the generator of V_{ov} is not affected by the currents used, the rate of change of potential at spike peak with current measures membrane resistance R_s at the peak of the spike, i.e.

$$dV_{ov}/dI = R_s.$$

The spike height V_s, which is the only measurable quantity with the method employed, is $V_{ov}-V_m$; therefore,

$$dV_s/dI = R_m - R_s.$$

The height of antidromic spikes has been plotted in Fig. 5 as a function of current. In this plot the peaks of the spikes have been aligned horizontally. The slope of the line through the points is equal to R_m-R_s. Since R_s is probably small in comparison with R_m the measured slope will be only a little smaller than R_m.

TABLE 1

Moto-neurone*	Rheobase $\times 10^{-9}$ A	Anti-dromic block† $\times 10^{-9}$ A	Synaptic potential (V_m-V_{th}) (mV)	Spike (V_s) (mV)	Time constant‡, of strength-latency curves (msec)	$\frac{d(V_m-V_{th})}{dI}$ § $=R_m-R_{th}$ (MΩ)	$\frac{dV_s}{dI}$ ‖ $=R_m-R_s$ (MΩ)
(1)	(2)	(3)	(4)	(5)	(6)	(7)	(8)
1	10·4	7·7	—	74·5	—	—	0·72
2	11·4	9·7	—	102·0	—	—	0·80
3	4·4	—	7·5	70·0	1·08	1·70	1·70
4	3·2	—	3·5	75·0	—	2·25	2·50
5	12·1	1·8	—	92·0	—	—	1·12
6	4·0	—	6·0	70·0	—	1·18	1·30
7	2·5	—	5·0	72·7	1·15	2·00	—
8	2·4	—	6·0	79·0	—	2·35	2·35
9	8·1	—	5·0	78·0	—	0·62	—
10	7·0	6·9	11·4	98·0	—	—	1·43
11	18·1	6·6	—	83·0	1·73	—	—
12	7·3	—	10·0	82·0	—	1·00	1·23
13	12·0	1·6	—	56·0	0·68	—	—
14	6·0	—	9·7	82·0	—	—	1·80
15	2·0	—	—	96·0	0·74	—	—
16	3·0	—	—	75·0	1·78	—	—
17	6·0	—	9·5	89·0	—	1·14	1·50
18	6·5	—	—	73·5	0·70	—	—
Av.	7·0	5·7	7·4	80·5	1·12	1·53	1·50
Av. of 52 units	7·4	5·5	7·4	78·9	1·08	1·66	1·65
Av. of 4 axons	1·7	—	—	79·5	0·27	—	—

* The 18 units listed are those for which at least three of the measurements indicated were available; only averages are shown for other measurements.

† Hyperpolarizing current required to produce 'partial block' of antidromic spike (see p. 455).

‡ Time constant of exponential curve best fitting experimental points of strength-latency or strength-duration plots (see Fig. 9).

§ Slope of plots of synaptic potentials against current (see Fig. 7).

‖ Slope of plots of spike height (V_s) against current (see Figs. 5 and 6).

Values of R_m-R_s observed in this manner are given in the last column of Table 1. They average 1·65 MΩ. This is the value of R_m if $R_s=0$ and thus represents a lower limit for R_m. Since R_s is probably less than 20% of R_m an upper limit for the average of R_m would be about 2·0 MΩ. The close

approximation of the points in the plot to a straight line indicates that $R_m - R_s$ does not change with I and therefore, most probably, that neither R_m nor R_s is affected by these currents. Moreover, since the straight-line relationship includes both positive and negative currents, the membrane shows no evidence of rectification with small currents.

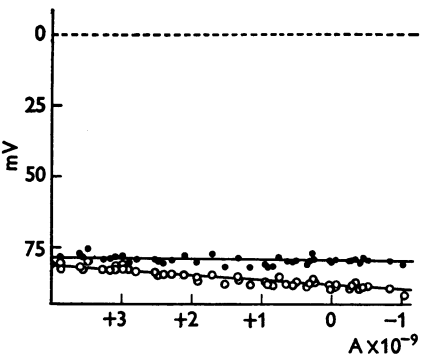

Fig. 6. Plot of orthodromic spike height V_s and potential difference between spike peaks and threshold inflexion $V_{ov} - V_{th}$ as a function of current through microelectrode. Potentials plotted downward as in Fig. 5. Positive current is outward directed. Data from records like those of Fig. 2. If spike peak potential is independent of current the open circles (○) represent membrane potential, V_m, and the slope of the line through them, 1·85 MΩ, gives the resting membrane resistance R_m. Similarly, line through filled circles (●), which has a slope of 0·25 MΩ, measures the rate of change of threshold membrane potential V_{th} with current.

Plots similar to that of Fig. 5 can be made for orthodromic rather than antidromic spikes (Fig. 6). As one would expect, similar values are obtained for $R_m - R_s$. In addition, the potential (V_{th}) at which the inflexion between synaptic potential and spike occurs, can be plotted on the same scales. The resulting points (filled circles of Fig. 6), fitted a straight line showing a small positive slope in the ten cases examined. This indicates that the recorded threshold polarization V_{th} is decreased by depolarizing and increased by hyperpolarizing currents. In the ten cases analysed for this purpose, the potential level recorded when firing occurred for synaptic excitation was 0–2·2 mV less negative than that calculated for direct excitation.

This change of threshold with currents has the dimensions of a resistance measuring 0·25 MΩ in the case illustrated and can be called R_{th}. It should be emphasized that the existence of a physical resistance of this value is not implied.

As previously discussed with relation to R_m, the measured slope of the threshold line should be increased by the magnitude of R_s. In the example of Fig. 6, $R_m - R_s = 1{\cdot}9$ MΩ. If $R_s \leqslant 0{\cdot}2\ R_m$ the true rate of change of threshold polarization with current, R_{th}, is between 0·25 and 0·72 MΩ. Since in all the

ten cases the slope of the threshold line was zero or positive it can be concluded that $R_{th} \geqslant R_s$.

Synaptic potential ($V_{th} - V_m$) *method.* Another method for measuring membrane resistance employs the variation of height of threshold synaptic potentials with current. With this method higher amplification can be used and thus greater precision is possible than with the former method based on spike height measurement.

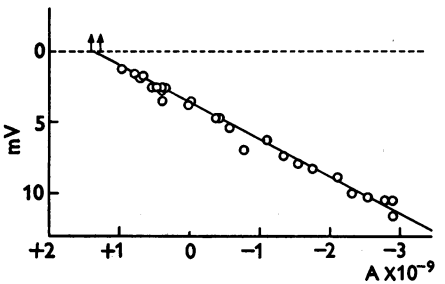

Fig. 7. Height of synaptic potential $V_m - V_{th}$ as a function of microelectrode current. Threshold inflexion points aligned horizontally (broken line) and synaptic potentials plotted downward. Data taken from high gain records which did not show spike peaks. The two arrows show two values of rheobasic current obtained in this experiment. Slope of line is 2·7 MΩ and measures $R_m - R_{th}$ (see Text).

The principle of the two methods is similar. The rate of change of resting polarization with current is equal to the resting membrane resistance:

$$dV_m/dI = R_m.$$

As said above, the rate of change of V_{th} with current has also the dimensions of a resistance and has been called R_{th}:

$$dV_{th}/dI = R_{th}.$$

If the measured synaptic potential $V_{th} - V_m$ is plotted against the current I, the resulting curve has a negative slope,

$$-\frac{d(V_{th} - V_m)}{dI} = R_m - R_{th}.$$

A typical plot of such data is shown in Fig. 7, in which synaptic potentials are plotted downward from the horizontal dashed line, as though the threshold polarization V_m were independent of current. The values of $R_m - R_{th}$ presented in column 7 of Table 1 show an average of 1·66 MΩ. This figure should not be compared with the average value of $R_m - R_s$ shown to be 1·65 MΩ in column 8, because different units were included in the two columns. The six units for which both measurements are available give average values of $R_m - R_s = 1{\cdot}76$ MΩ

and of $R_m - R_{th} = 1{\cdot}60$ MΩ. Again, assuming that the membrane resistance R_s at the peak of the spike is less than 20% of the resistance R_m of the resting membrane, the following ranges are obtained:

$$R_s \leqslant 0{\cdot}44 \text{ MΩ}, \quad 1{\cdot}76 \leqslant R_m \leqslant 2{\cdot}20 \text{ MΩ}, \quad 0{\cdot}16 \leqslant R_{th} \leqslant 0{\cdot}60 \text{ MΩ}.$$

Since, in the six units considered, $R_{th} - R_s$ has the average value of 0·16 MΩ while the average rheobasic current is $4{\cdot}56 \times 10^{-9}$ A, the average difference between threshold polarization, V_{th}, for direct or synaptic excitation measures 0·73 mV.

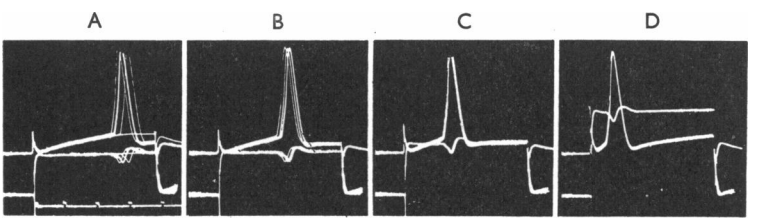

Fig. 8. Excitation by currents of different intensities. Lower beam measures current through microelectrode and upper beam records microelectrode potential. Ten sweeps are superimposed in each frame. In A, current is just above rheobase and occasionally fails to excite. With increasing current strength, latency is decreased and smaller latency variations occur. Time, 1 msec.

Strength-latency curve

Membrane time constant

It is well known (see Katz, 1939) that within limits a stimulating current pulse of long duration excites a nerve fibre with a current intensity lower than that required if the stimulus is shorter. The relation between intensity I and duration t of threshold stimulating currents is approximately described by the equation

$$I_{rh}/I = 1 - e^{-\frac{t}{\tau}},$$

where I_{rh} is rheobasic current and τ is the time constant.

Determination of the strength-duration relationship of threshold stimuli is a time-consuming procedure and was performed only occasionally in this study. Since the time available for making reliable measurements from inside motoneurones is often short it was considered more economical to determine the strength-latency relationship by measuring latency for impulse initiation following stimuli of long duration and different strengths.

While most measurements reported here are from strength-latency data, both methods were used for comparison of results. Fig. 8 shows typical records from which strength-latency data are taken. From such measurements plots are made of current strength against latency of firing and the theoretical curve is found which best fits the experimental points (Fig. 9). As shown in

Table 1, column 6, the time constants of these theoretical curves show an average value of 1·08 msec for 24 units tested.

Some confidence in the validity of these results obtained with microelectrodes is gained by applying the procedures described above to dorsal and ventral root fibres. Here the time constant was shorter than in somata, averaging 0·27 msec as shown in Table 1. This value corresponds to a chronaxie of 0·19 msec which is well within the range of chronaxies quoted in the literature for large nerve fibres of mammals (0·05–0·6 msec according to Schaefer, 1940, Table 18).

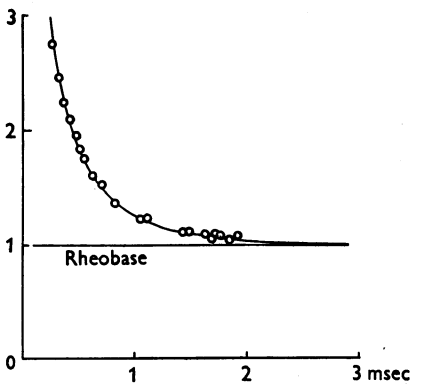

Fig. 9. Strength-latency relationship in a motoneurone. Plot of current intensity I, measured in terms of rheobase, as a function of spike latency t. Points taken from records like those of Fig. 8. The solid line is the best fitting theoretical curve from the equation mentioned in the text, and has a time constant $\tau = 0{\cdot}64$ msec.

Potential and excitability changes

Strength-latency curves can be obtained without difficulty with the methods employed in this research, and their time constants are consistent in different units. However, it cannot be assumed that the course of a strength-latency curve gives an accurate measure of the time-constant of the membrane since such events as accommodation and subthreshold responses might be complicating factors (see Hodgkin & Rushton, 1946). Therefore, the time-constant of the strength-latency curve has been compared in a given unit to the course of excitability and potential changes which follow abrupt onset or cessation of a stimulus.

Techniques of this type have often been applied to nerve fibres. Kries & Sewall (1881), Gildemeister (1908), Lucas (1910), Rushton (1932), Katz (1937), and others reported the time-course of excitability changes, whereas Hodgkin (1937, 1938), Hodgkin & Rushton (1946), Katz (1947), and others analysed the course of local potential changes following application of currents.

Similar measurements have been performed on motoneurones only recently. Araki & Otani (1955) recorded the bridge unbalance evoked by current pulses of long duration. With the electrode

outside a cell, the bridge was balanced for the applied currents. After penetration the same currents unbalanced the bridge and the time-course of this unbalanced potential was taken as a measure of the time constant of the penetrated unit. Eccles (1946, 1952), Brock, Coombs & Eccles (1952) and Coombs, Eccles & Fatt (1955*b*), on the other hand, based their measurements on the assumption that rate of decay of excitatory or inhibitory synaptic potentials is a measure of the time constant of motoneurone membranes.

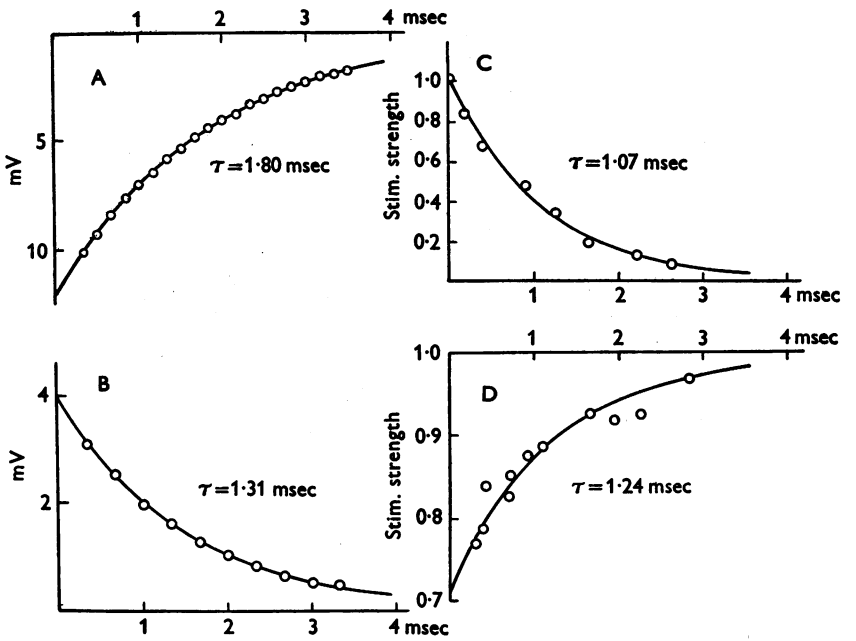

Fig. 10. Plots of potential and excitability changes obtained in one unit (unit 1 of Table 2). Open circles (○) are experimental measurements and solid lines are the best fitting exponential curves. A: course of bridge unbalance recorded after onset of a long depolarizing current; time constant, 1·80 msec. B: course of bridge unbalance following termination of a short depolarizing current; time constant 1·31 msec. C: excitability after onset of long depolarizing current; ordinate, strength of test stimulus required to excite, expressed as a fraction of its threshold strength in the absence of 'conditioning' current; time constant, 1·07 msec. D: excitability following termination of a short depolarizing current; ordinate as in C; time constant: 1·24 msec. In this unit, time constant was independent of current intensity up to 90% of threshold.

In the present research the following measurements have been made in addition to measurement of the strength-latency relationship:

(*a*) Potentials recorded during and following long (2–100 msec) hyperpolarizing or depolarizing current pulses.

(*b*) Excitability during and following the same long pulses.

(*c*) Potentials recorded following short (0·2–0·3 msec) hyperpolarizing or depolarizing current pulses.

(*d*) Excitability following the same short pulses.

Because accurate comparison of time constants determined in a unit by several different methods is a time-consuming procedure, this analysis was limited to two units only. The results obtained in these two units are illustrated in Fig. 10 and summarized in Table 2. Although it appears there that the values found with the various methods employed are in reasonably good agreement, some discussion is required.

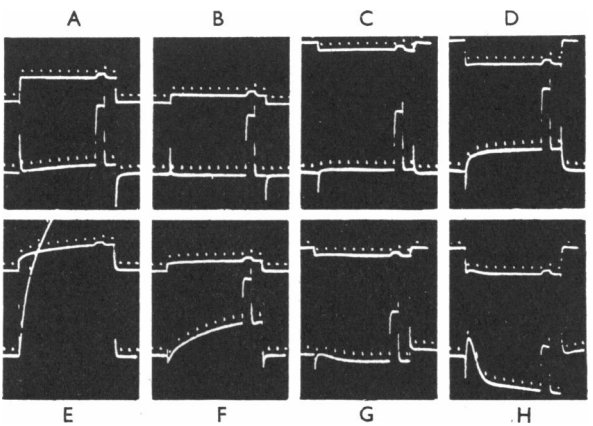

Fig. 11. Effects of currents on microelectrode. Measurements were made using the circuit of Fig. 1. The microelectrode was immersed in a bath of saline or 3 M-KCl which was connected to the bridge by the indifferent electrode I.E. Upper trace: current measured as in Fig. 1 B. Lower trace: microelectrode potential with respect to ground. Calibrating pulse, 50 mV: A–D, 3 M-KCl bath; E–H, saline bath. Values of electrode resistance and current intensities at start of pulse are as follows:

		A	B	C	D	E	F	G	H
Resistance (MΩ)		6	5	6	5	—	24	17	23
Current $\times 10^{-9}$ A	Initial	+44	+16	−15	−46	+22	+14	−14	−44
	Final	+45	+16	−15	−44	+46	+22	−14	−50

Positive sign indicates outward current. Note different time course of bridge unbalance with similar currents but different electrode resistance, for instance in B and F.

Bridge unbalance. It should be mentioned first that some of the measurements of the potentials recorded during current flow were recognized to be in error and were therefore discarded. Control experiments performed with the microelectrode dipped in salt solution (Fig. 11) showed that current flow often evokes an apparent change of electrode resistance (electrode polarization). This change results in gradual development of bridge unbalance and is recorded as a potential change often showing an approximately exponential time-course. Both size and time course of this change were observed to vary with electrode resistance as well as with current intensity. Its time constant, however, was generally much longer than that ascribable to the motoneurone membrane, amounting to about 5 msec in several cases. It can be suspected,

therefore, that the time constant of electrode changes may interfere with measurements of membrane time constant based on the time course of recorded potentials elicited by currents. The errors introduced by electrode polarization may be negligible when relatively coarse pipettes and weak currents are used, but is often very considerable in other cases. Interference by electrode polarization may be recognized when a measurement of time constant by bridge unbalance is widely different from measurements by other methods performed on the same cell and when the aberrant time constant is in the range of polarization time constants previously encountered *in vitro*.

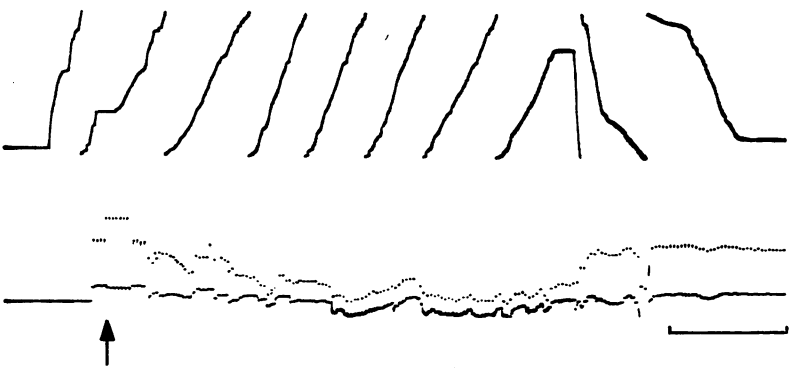

Fig. 12. Changes of electrode resistance with movement through the cord. Upper trace signals electrode movement; a full deflexion of the instrument is reached by a movement of 200 μ, after which the pen jumps back and begins recording of further movement in the same way. Lower trace, microelectrode potential with respect to ground led off as in Fig. 1. Calibration signals of 50 mV are delivered while the electrode is moved through the cord as indicated in the upper trace. Electrode resistance was 24 MΩ at ↑ as measured by disconnecting R_3 of Fig. 1A. Decrease of size of the recorded signal denotes increased electrode resistance (see p. 452). Time 30 sec.

It has been mentioned that electrode polarization elicited by a given current is different with different electrode resistances. It was further observed that electrode resistance may change quite extensively with even minute movements of the electrode in nervous tissue (Fig. 12). For these reasons the bridge unbalance elicited by a given current was often different in size and time-course if the electrode was moved in the cord. In particular, it was sometimes found that rate of development of bridge unbalance was slower with the electrode outside than inside a motoneurone. This result could be attributed to change of resistance of the electrode consequent to the small movement required to shift its tip from inside to outside a unit and showed that the course of bridge unbalance during current flow may be an unreliable measure of membrane time constant even when records taken inside and outside a unit are compared. Valid results can be obtained with this method only when it can be ascertained that electrode polarization is negligible.

Accommodation. Time constant of strength-latency curves would be appreciably shorter than membrane time constant if spinal motoneurones of anaesthetized preparations presented accommodation comparable to that of peripheral nerves. Accommodation of motoneurones was not studied systematically. In three units, however, accommodation to depolarizing currents was studied by testing excitability during a current pulse lasting 100 msec. A typical result is illustrated in Fig. 13 which shows that accommodation is much less prominent in motoneurones than in peripheral nerves (cf. Rushton, 1932) and probably does not introduce a serious error in membrane time-constant measurements based on strength-latency curves. Other

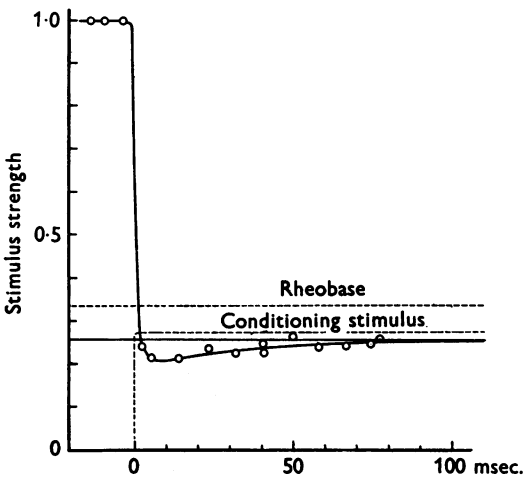

Fig. 13. Accommodation to long depolarizing current. Ordinate, current intensity expressed in fractions of threshold intensity of a test stimulus of 0·2 msec duration. Broken lines indicate, on the same scale, intensity of long-lasting (conditioning) current used during the experiment, and its rheobase value.

limitations may be inherent to the strength-latency method, but it would be premature to discuss these at this time.

Excitability. The last method employed, consisting of tracing the course of excitability changes induced by abrupt stimuli, is not subject to many of the defects of other methods but proved to be too laborious for practical purposes. Usually, for the sake of speed of experimentation, the curves obtained by this method were of necessity based on relatively few points only and thus were less accurate than those obtained by the other methods mentioned. In favourable conditions, however, the results obtained by excitability measurement may be regarded as reliable.

Validity of results. In an attempt to reveal sources of error peculiar to any one of the methods employed, the results have been averaged in different ways, as shown in Table 2 B. It might be thought that the time-constant as measured

by excitability would be different from that using potential measurements since electrode polarization effects would be eliminated. Similarly, methods using hyperpolarization would be free of the possible non-linearities of the 'local response'. And finally results with short current pulses would be uncontaminated by accommodation. Comparison of results grouped in these various ways in Table 2 shows, however, that differences in results by the different methods are masked by randomness of the individual measurements.

TABLE 2. Determination of τ (msec) by different methods

A

Method	Unit 1	Unit 2	Method	Unit 1	Unit 2
Potential following short depolarization	1·31	1·01	Excitability following short depolarization	1·24	1·25
Potential following short hyperpolarization	1·49	1·06	Excitability following short hyperpolarization	0·97	1·00
Potential during long depolarization	1·83	1·33	Excitability during long depolarization	0·71	1·15
Potential during long hyperpolarization	1·43	1·51	Excitability during long hyperpolarization	1·26	1·74
Potential following long depolarization	0·85	—	Excitability following long depolarization	0·70	—
Potential following long hyperpolarization	1·23	—	Excitability following long hyperpolarization	1·22	—

B

Method	Unit 1	Unit 2	Unit 1 + unit 2	Method	Unit 1	Unit 2	Unit 1 + unit 2
Potential	1·36	1·23	1·30	Excitability	0·97	1·28	1·04
Hyperpolarization	1·27	1·32	1·28	Depolarization	1·08	1·18	1·12
Long currents	1·12	1·44	1·20	Short currents	1·26	1·07	1·14

	Unit 1	Unit 2	Unit 1 + unit 2
Av. of all values but strength-latency	1·14	1·25	1·18
Strength-latency	0·76	1·02	0·88
Av. of all values	1·09	1·21	1·14

These random errors might be reduced in the average of all values, and it will be noted that the average figure of 1·18 msec resulting from 44 measurements of excitability and potential in two units is quite comparable to the value of 1·08 msec derived from averaging the strength-latency measurements performed in the different units of Table 1. It will be noted, however, that in the two units of Table 2 the time-constant value obtained by strength-latency measurements (0·88 msec) is considerably lower than the average value obtained with other methods (1·18 msec). If the results obtained in these two units are representative, it must be concluded that strength-latency measurements give time constant values shorter than other methods and that a higher average figure (perhaps 1·4 msec) would have been found if time constant had been analysed in all units with the different methods described.

Technical limitations

It is well known that the properties of impaled elements often change rapidly with time. In a previous study (Frank & Fuortes, 1955) the changes in the potentials recorded from a unit were the main indication of the condition of the unit itself, and it was noted that not only deterioration but also improvement could occur with time. In the present study changes of electrical properties of motoneurones could be demonstrated to occur also in the absence of major changes of spike potential. More often both spike potential and excitability changed with time but no systematic relations between the two were found. One example of changes occurring with time in one unit is given in Fig. 14. This example is given as an illustration of the limitations of techniques involving impalement of neural elements and may explain why measurements requiring long times were rarely performed.

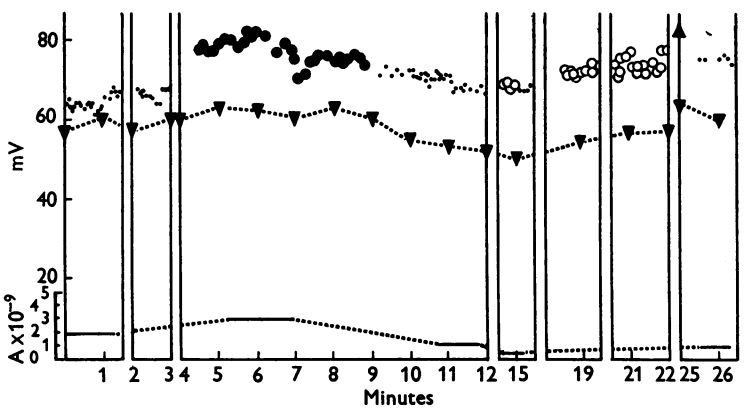

Fig. 14. Changes occurring in a penetrated motoneurone. Unconnected points show height of spikes V_s for different routes of excitation. •, excitation with long current pulses through microelectrode; ●, excitation with brief current pulses through microelectrode; ○, antidromic excitation; ▲, orthodromic excitation; ▼, membrane potential. Solid bars connected by dotted lines, rheobasic current. Abscissa: time after penetration. Discontinuities indicate periods when no data were recorded.

DISCUSSION

The electrical properties found in the motoneurones examined are generally consistent with those established for other nerve tissues. Assuming with Eccles (1956), that the surface area of a motoneurone is 5×10^{-4} cm^2, resistivity of the motoneurone membrane is about 1000 Ω cm^2 and thus is of the same order of magnitude as the resistivity of non-medullated nerves (cf. Weidmann, 1956, table 3).

The finding that excitation by applied currents occurs when there is about 1 mV more average membrane depolarization than for synaptic excitation

requires some discussion. Several interpretations can be offered to explain this result. One possibility is that synaptic bombardment not only evokes depolarization of the motoneurone membrane as recorded in the synaptic potential, but also exerts an additional excitatory action which is not revealed by the physical measurements performed. Views of this type have often been expressed in the past, and some authors (Lloyd, 1955; Lloyd, Hunt & McIntyre, 1955; Hunt, 1955) still postulate that two separate events occur at excitatory synapses; one brief, unrelated to the synaptic potential and capable of exciting and a second longer lasting, closely associated to the synaptic potential but only capable of facilitating excitation. This interpretation has the disadvantage of postulating an excitatory action not measured or defined in physical terms.

Interpretations not subject to this limitation can be proposed. An intracellular microelectrode records the average polarization of different parts of the cell membrane. It can be thought, and indeed it is quite likely, that the depolarization evoked by synaptic or direct stimuli is not uniformly distributed over the whole membrane. Therefore some areas of the motoneurone membrane will be more and some will be less polarized than the recorded average. If the geometrical distribution of the depolarization with respect to the locus where the spike is initiated is systematically different for direct and synaptic excitation, a consistent difference would be found in the average depolarization recorded in the two cases.

This interpretation implies that a propagated discharge of the motoneurone soma begins at some particular locus. This is supported by the finding that motoneurone spikes develop in two steps (Araki & Otani, 1955; Eccles, 1956; Fatt, 1956; Fuortes, Frank, Becker & Morrell, 1956). For direct excitation there is good evidence that the locus of origin of the spike is in the neighbourhood of the axon and propagates from there orthodromically along the axon itself and 'antidromically' over the rest of the cell (Fuortes *et al.* 1956). It has been suggested (Araki & Otani, 1955; Eccles, 1956; Fatt, 1956) that these same processes occur for synaptic excitation, but the evidence so far is perhaps not equally conclusive.

Thus the results just quoted fulfil one of the basic requirements of the proposed interpretation, namely, that the spike is initiated at a particular locus of the cell membrane. Therefore, the hypothesis that synaptic or direct excitation of a motoneurone occurs when some part of its membrane is depolarized to a threshold value is tenable and appears to be testable by available techniques.

The other result deserving brief discussion refers to measurement of the time constant of the motoneurone membrane. It has been pointed out above that the average value of 1·08 msec obtained from strength-latency measurements should perhaps be corrected to 1·4 msec. From these values, and from

the measurements of area and of resistance given above, values of 1·0–1·5 μF/cm^2 are obtained for the motoneurone membrane. These figures are lower than those found by Araki & Otani (1955) in toads' motoneurones, but it cannot be assessed whether this difference should be ascribed to species difference or to differences of technique. More important is comparison between the values obtained in this study and the conclusion reached by Eccles (1952), Brock *et al.* (1952), and others, that the time constant of motoneurones of cats amounts to 4 msec. This conclusion was based on evidence showing that orthodromic volleys producing a normal synaptic potential in a resting motoneurone fail to evoke any change if they arrive in coincidence with an action potential of antidromic origin. This was considered to demonstrate that the action exerted by an impinging volley is short-lasting and that the falling phase of the synaptic potential reflects passive electrical properties of the post-synaptic membrane.

The present results, confirmed by more recent results obtained in Eccles's laboratory (Eccles, 1956), suggest instead that the long duration of the potential change evoked in the motoneurone soma membrane is not a consequence of the long time constant of this membrane itself, but rather of a similarly long-lasting change occurring elsewhere.

SUMMARY

1. Electrical properties of spinal motoneurones have been measured in anaesthetized cats. Potential changes occurring across the motoneurone membrane were led off by means of micropipettes inserted inside the neurone soma. Stimulating currents were delivered through the same micropipette used for recording and a Wheatstone bridge was used for balancing the potential drop developed across the microelectrode resistance by the stimulating current.

2. All penetrated units could be excited by depolarizing currents of sufficient intensity. Depolarizing currents insufficient to excite facilitated the action of orthodromic stimuli as well as antidromic invasion of motoneurones. Hyperpolarizing currents exerted opposite effects. The average rheobase was $7{\cdot}4 \times 10^{-9}$ A.

3. Total resistance of the motoneurone membrane was measured by two indirect methods based on the assumption that the overshoot potential is not affected by polarizing currents and was found to measure 1·65 MΩ in the average. The same methods and the same assumption were used for determining the amount of depolarization required to elicit firing by direct application of electrical stimuli. In the average of six units this was 0·73 mV greater than the depolarization evoked in the same units by a threshold synaptic potential.

4. Strength-latency curves were plotted for twenty-four motoneurones and showed an average time constant of 1·08 msec. Accommodation (measured in three cases) was found to be much smaller than in peripheral nerves and

probably did not affect the time constant measured by the strength-latency method.

5. In order to test the significance of the time constant obtained from strength-latency curves its value was compared in two units to the time constant of potential and excitability changes following application of currents. In these two units the average value by strength-latency measurements was 0·88 msec as compared to an average value of 1·18 msec by potential and excitability measurements.

6. The results lead to the conclusion that motoneurone excitation occurs when its membrane is depolarized to a threshold potential. A possible interpretation of the finding that the recorded threshold potential is slightly less negative for direct than for synaptic excitation is discussed. With this interpretation it is unnecessary to assume that impinging impulses evoke motoneurone firing by any process other than by depolarization of the membrane to a critical level.

7. Since the time constant determined by strength-latency curve, potential, or excitability changes is considerably shorter than the time constant of decay of the synaptic potential, it is improbable that the long duration of the falling phase of synaptic potentials is due exclusively to the time constant of the motoneurone soma membrane.

REFERENCES

ARAKI, T. & OTANI, T. (1955). Response of single motoneurons to direct stimulation in toad's spinal cord. *J. Neurophysiol.* **18**, 472–485.

BROCK, L. G., COOMBS, J. S. & ECCLES, J. C. (1952). The nature of the monosynaptic excitatory and inhibitory processes in the spinal cord. *Proc. Roy. Soc.* B, **140**, 169–176.

BROCK, L. G., COOMBS, J. S. & ECCLES, J. C. (1953). Intracellular recording from antidromically activated motoneurones. *J. Physiol.* **122**, 429–461.

COOMBS, J. S., ECCLES, J. C. & FATT, P. (1955*a*). The electrical properties of the motoneurone membrane. *J. Physiol.* **130**, 291–325.

COOMBS, J. S., ECCLES, J. C. & FATT, P. (1955*b*). Excitatory synaptic action in motoneurones. *J. Physiol.* **130**, 374–395.

ECCLES, J. C. (1946). Synaptic potentials of motoneurones. *J. Neurophysiol.* **9**, 87–120.

ECCLES, J. C. (1952). The electrophysiological properties of the motoneurone. *Cold Spr. Harb. Symp. quant. Biol.* **17**, 175–183.

ECCLES, J. C. (1956). *Physiology of Nerve Cells* (in the Press).

FATT, P. (1956). Mode of activation of the motoneurone. *J. Physiol.* (in the Press).

FRANK, K. & FUORTES, M. G. F. (1955). Potentials recorded from the spinal cord with microelectrodes. *J. Physiol.* **130**, 625–654.

FUORTES, M. G. F., FRANK, K., BECKER, M. C. & MORRELL, R. M. Steps in the development of motoneurone spikes. *Abstr. XX int. physiol. Congr., Bruxelles*, 1956, pp. 316–317.

GILDEMEISTER, M. (1908). Über Interferenzen zwischen zwei schwachen Reizen. *Pflüg. Arch. ges. Physiol.* **124**, 447–461.

HODGKIN, A. L. (1937). A local electric response in crustacean nerve. *J. Physiol.* **91**, 5–7*P*.

HODGKIN, A. L. (1938). The subthreshold potentials in a crustacean nerve fibre. *Proc. Roy. Soc.* B, **126**, 87–121.

HODGKIN, A. L. & RUSHTON, W. A. H. (1946). The electrical constants of a crustacean nerve fibre. *Proc. Roy. Soc.* B, **133**, 444–479.

HUNT, C. C. (1955). Monosynaptic reflex response of spinal motoneurons to graded afferent stimulation. *J. gen. Physiol.* **38**, 813–852.

KATZ, B. (1937). Experimental evidence for a non-conducted response of nerve to subthreshold stimulation. *Proc. Roy. Soc.* B. **835**. 244–276.

KATZ, B. (1939). *Electric Excitation of Nerve.* London: Oxford University Press.

KATZ, B. (1947). Subthreshold potentials in medullated nerve. *J. Physiol.* **106**, 66–79.

KRIES, J. v. & SEWALL, H. (1881). Ueber die Summierung untermaximaler Reize in Muskeln und Nerven. *Arch. Anat. Physiol., Lpz.*, **1881**, 66–77.

LLOYD, D. P. C. (1955). Intracellular transmission. In Howell's *Textbook of Physiology*, 17th ed. Ed. Fulton, J. F. Philadelphia: Saunders.

LLOYD, D. P. C., HUNT, C. C. & MCINTYRE, A. K. (1955). Transmission in fractionated monosynaptic spinal system. *J. gen. Physiol.* **38**, 307–317.

LUCAS, K. (1910). Quantitative researches on the summation of inadequate stimuli in muscle and nerve with observations on the time factor in electrical excitation. *J. Physiol.* **39**, 461–475.

MACNICHOL, JR., E. F. & WAGNER, H. G. (1954). A high impedance input circuit suitable for electrophysiological recording from micropipette electrodes. *Nav. med. res. Inst.* **12**, 97–118.

RUSHTON, W. A. H. (1932). A new observation in the excitation of nerve and muscle. *J. Physiol.* **75**, 16–17*P*.

SCHAEFER, H. (1940). *Elektrophysiologie*, Vol. 1. Wien: Deuticke.

SOLMS, S. J., NASTUK, W. L. & ALEXANDER, J. T. (1953). Development of a high fidelity preamplifier for use in the recording of bioelectric potentials with intracellular electrodes. *Rev. sci. Instrum.* **24**, 960–967.

WEIDMANN, S. (1956). *Elektrophysiologie der Herzmuskelfaser.* Bern & Stuttgart: Huber.

WOODBURY, J. W. (1953). Recording central nervous system activity with intracellular ultramicroelectrodes: use of negative-capacity amplifier to improve transient response. *Fed. Proc.* **12**, 159.